Charge Separation in Donor-Chromophore-Acceptor Assemblies: Linkage and Driving Force Dependence of Photoinduced Electron Transfers

S. L. Larson,† C. Michael Elliott,* and D. F. Kelley*

Department of Chemistry, Colorado State University, Fort Collins, Colorado 80523-1872

Received: August 22, 1994; In Final Form: December 22, 1994[⊗]

A series of covalently linked Ru(bipyridine)$_3$-donor-acceptor complexes was prepared where the donor-to-chromophore and acceptor-to-chromophore methylene chain lengths were varied. Time-resolved absorption studies were performed to elucidate intramolecular electron transfer rates. The electron donor in the above series is a phenothiazine moiety linked to a bipyridine by a $(-CH_2-)_p$, $p = 3-8$ chain, and the electron acceptor is an *N,N'*-diquaternary-2,2'-bipyridinium moiety linked to a bipyridine by a $(-CH_2-)_m$, $m = 2$, 3, 4 chain. Oxidative quenching of the Ru(bipyridine)$_3$ metal-to-ligand charge transfer (MLCT) state followed by phenothiazine-to-ruthenium electron transfer resulted in a long-lived charge-separated state. A wavelength-dependent excitation resulted in a slowly decaying absorption which is assigned to the excited-state phenothiazine. The magnitude of this component in the transient absorption serves as an internal standard for determining relative quantum yield for formation of the charge-separated state. Marcus inverted region behavior was observed in back electron transfer. Rate constants for electron transfer from phenothiazine to Ru(III) decreased as the length of the bridging chain increased from $p = 4$ to 8. Chain length independence of the back electron transfer rate in the series of complexes with varied chromophore-acceptor distances ($m = 2$, 3, and 4) suggests the formation of an association complex during oxidative quenching of MLCT state and argues against a σ-bond superexchange pathway for back electron transfer.

Introduction

Photoinduced electron transfer reactions are of fundamental interest and practical importance. It is by such reactions, through the process of photosynthesis, that nature converts sunlight into chemical energy. Interest in synthetic systems which mimic the initial charge separation steps in photosynthesis is longstanding.[1,2] The ultimate motivation in these studies is to exploit the potential ability of nonbiological systems to convert optical energy and store it as useful chemical products. Two general approaches have been employed in pursuing this problem. Almost all of the early work involved schemes utilizing intermolecular electron transfers (ET) between optically excited chromophores and some combination of electron donors and acceptors in solution. Several such bimolecular schemes were shown to be capable of storing some fraction of the incident optical energy, at least, transiently (nano- to microseconds).[1-3] Alternatively, this intermolecular step can be avoided by constructing more complex triad assemblies in which an electron donor and acceptor are both present.[4-7] These linked donor-chromophore-acceptor (D-C-A) systems are often capable of generating long-lived (hundreds of nanoseconds) photoinduced charge-separated (CS) states with good quantum yields. Both the quantum yield for formation and the lifetime of the CS state formed in D-C-A triad assemblies are expected to be strongly dependent on the structure of the assembly (e.g., the linkages) and the energetics of the various electron transfer steps.

In this paper we report results from time-resolved spectroscopic studies of a series of donor-chromophore-acceptor systems, based on a substituted ruthenium(II) tris(bipyridine) ($Ru(bpy)_3^{2+}$) chromophore, covalently attached by flexible polymethylene chains to an *N,N'*-diquaternary-2,2'-bipyridinium salt (diquat, DQ^{2+}) electron acceptor and to two phenothiazine (PTZ) electron donors. An example structure is shown in Figure 1. Photoexcitation of these complexes in low-polarity solvents produces a long-lived charge-separated state in which one of the PTZs is oxidized, the diquat is reduced, and the $Ru(bpy)_3^{2+}$ chromophore is returned to the ground state. The identity of the CS state has been confirmed previously using transient absorption spectroscopy.[4,5]

We have recently reported time-resolved emission studies on a subset of the D-C-A complexes under investigation here.[4] This study partially elucidated the mechanism by which the CS state is formed. The chromophore, $Ru(bpy)_3^{2+}$, absorbs light and is excited into its metal-to-ligand charge transfer (MLCT) state. This species is best described as $[Ru^{III}(bpy)_2(bpy^{\bullet-})]^{2+}$, in which a d-electron from the metal has been excited to a π^*-orbital localized on one of the bipyridines. In this excited state, $Ru(bpy)^{2+*}$ is both a stronger oxidizing agent and a stronger reducing agent than is the ground-state complex; consequently, it is subject to either oxidative or reductive quenching of the MLCT emission. When an electron acceptor is present, the unpaired electron of $bpy^{\bullet-}$ can be transferred to the acceptor. In the presence of a donor, an electron can be transferred from the donor to the unoccupied metal d-orbital. Comparison of the electron-transfer rates from the MLCT state for analogous chromophore-acceptor diad and donor-chromophore-acceptor triad complexes has shown that the initial electron-transfer step, in all cases, is from $bpy^{\bullet-}$ to diquat.[4,5] Diad complexes containing only PTZ donors linked to the $Ru(bpy)_3^{2+}$ chromophore show emission quenching on a much longer (100-300 ns) time scale.[8]

In order to further understand the formation of the charge-separated state in these systems, we have measured the appearance kinetics of the oxidized donor (PTZ^+) and the reduced acceptor (DQ^+) following MLCT excitation in three series of D-C-A complexes. The D-C-A complexes studied (see Figure 1) have the general form [Ru(4*p*-PTZ)$_2$(4*mn*-

* Authors to whom correspondence should be addressed.
† Current address: U.S. Army Corps of Engineers, Waterways Experiment Station, Vicksburg, MS.
⊗ Abstract published in *Advance ACS Abstracts,* April 1, 1995.

0022-3654/95/2099-6530$09.00/0

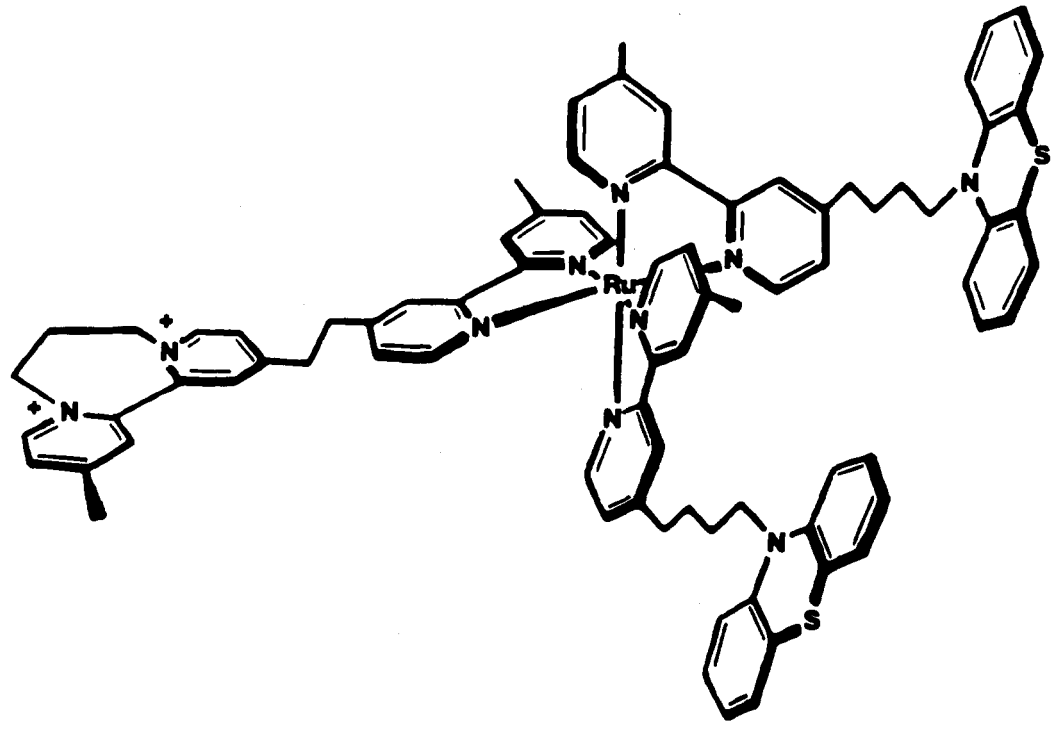

Figure 1. Donor–chromophore–acceptor complex, Ru(44-PTZ)$_2$423-DQ^{2+}.

DQ^{2+})]$^{4+}$. 4*p*-PTZ is a phenothiazine-containing ligand, (*N*-phenothiazinato) linked at the 4′ position to a 4-methyl-2,2′-bipyridine via a methylene chain (length *p*). The electron-accepting ligand consists of a bipyridine moiety which is methylated at the 4-position, linked at the 4′-position via a methylene chain of length *m* to a diquat. The pyridinium nitrogens of the diquat are linked by a methylene chain of length *n*. In this work *p* is 3–8, *m* is 2, 3, or 4, and *n* is 3 or 4. Thus the values of *p* and *m* determine the fully extended distance between the chromophore and the PTZ donor and the DQ^{2+} acceptor, respectively. The value of *n* determines the reduction potential of the DQ^{2+} and, thus, the exothermicity of electron transfers involving the DQ^{2+}.

Experimental Section

Electrochemical Measurements. All electrochemical measurements were carried out in O_2-free, nitrogen-purged acetonitrile solutions with 0.1 M tetra-*n*-butylammonium hexafluorophosphate ($TBAPF_6$) as supporting electrolyte. A conventional three-electrode cell was used with a glassy carbon working electrode, a platinum wire loop auxiliary electrode, and a saturated calomel electrode (SCE) as reference. Cyclic voltammetry was performed on a PAR Model 173 potentiostat.

Materials. All reagents and solvents were purchased commercially and used without further purification unless noted. $TBAPF_6$ was prepared as previously reported,[9] recrystallized three times from hot ethanol, and dried under vacuum. 4,4′-Dimethyl-2,2′-bipyridine (DMB) was recrystallized from ethyl acetate before use (melting point 172–177 °C). The eluent for thin layer chromatography (TLC) was a 50% acetonitrile, 40% water, and 10% saturated aqueous KNO_3 solution (by volume).

4-Methyl-4′-(4-(*N*-phenothiazinato)propyl)-2,2′-bipyridine (43-PTZ) (II). 4,4′-Dimethyl-2,2′-bipyridine (Reilly Tar and Chemical, Indianapolis) (10 g) which had previously been dried under vacuum, was dissolved in 250 mL of THF (freshly distilled from Na/benzophenone). This solution was added, over the course of 1 h, to a previously prepared solution of LDA in THF (8 mL of freshly distilled diisopropylamine, 24.7 mL of 2.2 M butyllithium in 25 mL of dry THF maintained at −78 °C). The dark brown solution was stirred under N_2 and maintained at −78 °C (dry ice/acetone) for 2.5 h. A 10-fold excess (50 g) of ethylene glycol di-*p*-tosylate dissolved in 350 mL of THF was then added to the reaction which was stirred at −78 °C for an additional hour. The dry ice bath was then removed and the solution allowed to warm to room temperature (1.5 h). During this period, the solution changed first to a dark green color, and finally to yellow. The reaction was then quenched by the addition of 150 mL of H_2O. The solution was extracted with 1 × 100 mL of ether and 2 × 100 mL of CH_2Cl_2. All of the organic fractions were combined and the volume was reduced by rotary evaporation to approximately 200 mL. This solution was filtered and chromatographed on a 60–200 mesh, grade 62 silica gel column (W. R. Grace) eluting first with CH_2Cl_2 followed by 4% acetone/CH_2Cl_2. The eluent containing the intermediate product, 4-methyl-4-(4-tosylpropyl)-2,2′-bipyridine (**I**), was concentrated by rotary evaporation and chromatographed again using 2% acetone/CH_2Cl_2. After removal of the solvent, **I** was obtained as a white oil which was determined to be pure by TLC. The yield of **I** was determined to be 35%.

Freshly recrystallized (from benzene) phenothiazine (PTZ) (2.0 g) was placed in a 100 mL round-bottomed flask in a ice/water bath, under N_2, in 30 mL of dry THF. Sodium hydride (0.35 g), 50% dispersion in oil, was added and the resulting gold-colored solution was stirred for 2 h before a THF solution (approximately 20 mL) containing 1.2 g of **I** was added dropwise. The ice/water bath was removed and the solution was allowed to stir for 2 h; a reflux condenser was attached and the solution was heated to reflux for 12 h. The reaction was then quenched with 50 mL of water and the solution extracted with 2 × 25 mL portions of ether and 2 × 25 mL portions of CH_2Cl_2. The combined organic solutions were dried with anhydrous Na_2CO_3 and the solvent was removed by rotary evaporation to yield a gold-colored oil. The crude product was chromatographed on silica gel, eluting first with CH_2Cl_2 to

remove unreacted PTZ followed by 4% acetone/CH_2Cl_2 which eluted the product, 43-PTZ, **II**, as a light peach-colored solution. The solution was rotary evaporated and the resulting oil dissolved in a minimum of hot ethanol, filtered, and placed in the freezer for 2 days. The ethanol was decanted from the colorless oily residue which was dried under vacuum. Cyclic voltammetry of **II** in acetonitrile showed a reversible wave for the $PTZ^{0/+}$ couple at 0.74 V vs SCE.

^1H NMR (200 MHz $CDCl_3$): δ 1.60−1.70 (2 H), 2.45 (3 H), 2.60−2.80 (2 H), 3.75−3.90 (2 H), 6.70−6.90 (6 H), 7.05−7.20 (4 H), 8.20−8.30 (2 H) and 8.40−8.60 (2 H) ppm.

Methyl-4′-(4-(*N*-phenothiazinato)butyl)-2,2′-bipyridine (44-PTZ) (III). This ligand was prepared in an analogous fashion to **II** above except that 1,3-dibromopropane (10× excess Aldrich) was substituted for the ethylene glycol di-*p*-tosylate. Following the final chromatography steps the solution was rotary evaporated and the resulting oil dissolved in a minimum of hot ethanol, filtered, and placed in the freezer for 2 days. The solid 44-PTZ product was collected by filtration and dried under vacuum (melting point 93−98 °C). Cyclic voltammetry of **III** in acetonitrile showed a reversible wave for the $PTZ^{0/+}$ couple at 0.70 V vs SCE.

^1H NMR (200 MHz $CDCl_3$): δ 1.60−1.70 (4 H), 2.45 (3 H), 2.60−2.80 (2 H), 3.75−3.90 (2 H), 6.70−6.90 (6 H), 7.05−7.20 (4 H), 8.20−8.30 (2 H), and 8.40−8.60 (2 H).

4-Methyl-4′-(4-(*N*-phenothiazinato)pentyl)-2,2′-bipyridine (45-PTZ) (IV). This compound was prepared as above except 1,4-dibromobutane was added instead of 1,3-dibromopropane. The oily residue obtained following decanting cold ethanol was vacuum dried. Cyclic voltammetry of **IV** in acetonitrile showed a reversible wave for the $PTZ^{0/+}$ couple at 0.70 V vs SCE.

^1H NMR (200 MHz $CDCl_3$): δ 1.30−1.50 (2 H), 1.60−1.70 (4 H), 2.45 (3 H), 2.60−2.80 (2 H), 3.75−3.90 (2 H), 6.70−6.90 (6 H), 7.05−7.20 (4 H), 8.20−8.30 (2 H), and 8.40−8.60 (2 H).

4-Methyl-4′-(4-(*N*-phenothiazinato)hexyl)-2,2′-bipyridine (46-PTZ) (V). This compound was prepared as above except 1,5-dibromopentane was added instead of 1,3-dibromopropane. The solid 46-PTZ was obtained by filtration (melting point 90−93 °C). Cyclic voltammetry of **V** in acetonitrile showed a reversible wave for the $PTZ^{0/+}$ couple at 0.70 V vs SCE.

^1H NMR (200 MHz $CDCl_3$): δ 1.30−1.50 (4 H), 1.60−.170 (4 H), 2.45 (3 H), 2.60−2.80 (2 H), 3.75−3.90 (2 H), 6.70−6.90 (6 H), 7.05−7.20 (4 H), 8.20−8.30 (2 H), and 8.40−8.60 (2 H).

4-Methyl-4′-(4-(*N*-phenothiazinato)heptyl)-2,2′-bipyridine (47-PTZ) (VI). This compound was prepared as above except 1,6-dibromohexane was added instead of 1,3-dibromopropane. The oily residue obtained following decanting cold ethanol was vacuum dried. Cyclic voltammetry of **VI** in acetonitrile showed a reversible wave for the $PTZ^{0/+}$ couple at 0.70 V vs SCE.

^1H NMR (200 MHz $CDCl_3$): δ 1.30−1.50 (6 H), 1.60−1.70 (4 H), 2.45 (3 H), 2.60−2.80 (2 H), 3.75−3.90 (2 H), 6.70−6.90 (6 H), 7.05−7.20 (4 H), 8.20−8.30 (2 H), and 8.40−8.60 (2 H).

4-Methyl-4′-(4-(*N*-phenothiazinato)octyl)-2,2′-bipyridine (48-PTZ) (VII). This compound was prepared as above except 1,7-dibromoheptane was added instead of 1,3-dibromopropane. The oily residue obtained following decanting cold ethanol was vacuum dried. Cyclic voltammetry of **VII** in acetonitrile showed a reversible wave for the $PTZ^{0/+}$ couple at 0.70 V vs SCE.

^1H NMR (200 MHz $CDCl_3$): δ 1.30−1.50 (8 H), 1.60−1.70 (4 H), 2.45 (3 H), 2.60−2.80 (2 H), 3.75−3.90 (2 H), 6.70−6.90 (6 H), 7.05−7.20 (4 H), 8.20−8.30 (2 H), and 8.40−8.60 (2 H).

***N*-Methylphenothiazine.** Freshly recrystallized (from benzene) phenothiazine (PTZ) (2.0 g) was placed in a 100 mL round-bottomed flask in an ice/water bath, under N_2, in 30 mL of dry THF. Sodium hydride (0.35 g), 50% dispersion in oil, was added and the resulting gold-colored solution was stirred for 2 h before a THF solution approximately 20 mL) containing 1 equiv of CH_3I was added, dropwise. The ice/water bath was removed and the solution was allowed to stir for 2 h. The reaction was then quenched with 50 mL of water and the solution extracted with 2 × 25 mL portions of ether and 2 × 25 mL portions of CH_2Cl_2. The combined organic solutions were dried with anhydrous Na_2CO_3 and the solvent was removed by rotary evaporation. The crude product was chromatographed on silica gel, eluting with cyclohexane and the fractions containing the methylphenothiazine combined and rechromatographed. The pure fractions (by TLC) were combined and rotary evaporated. The resulting solid was dissolved in a minimum of hot benzene, filtered, and placed in the freezer overnight. The ethanol was decanted from the colorless solid which was dried under vacuum. Cyclic voltammetry of *N*-methylphenothiazine in acetonitrile showed a reversible wave for the $PTZ^{0/+}$ couple at 0.70 V vs SCE.

^1H NMR (200 MHz $CDCl_3$): δ 3.85 (3 H), 6.70−6.90 (4 H), 7.05−7.20 (4 H).

Bis[4′-methyl[2,2′-bipyridyl]-4-yl]propane (VIII) and Bis-[4′-methyl[2,2′-bipyridyl]-4-yl]butane (IX). These straight-chain-linked bipyridines were synthesized as reported previously.[10]

Formation of $n = 4$ "Diquats" from VIII and IX. One of the two bipyridines in either of the compounds **VIII** and **IX** could be converted into the respective diquaternary salt (diquat) having four methylene units linking the two bipyridine nitrogens ($4m4\text{-}DQ^{2+}$) by reaction with 1,4-dibromobutane via procedures previously reported.[10] The purification and yield were similar to those previously reported.[10] After purification by chromatography on silica gel (eluent 40% H_2O−10% KNO_3 (aq satd)−50% acetonitrile (4:1:5) (vol)), the acetonitrile was removed at reduced pressure and the respective compounds were each isolated by precipitation as their PF_6^- salts. These compounds decompose at 160−190 °C (434) and 185−210 °C (444).

Bis(4*p*-PTZ)dichlororuthenium(II) ($Ru(4p\text{-}PTZ)_2Cl_2$) (X). LiCl (0.0563 g, 10 equiv) and 12 mL of reagent grade (T. J. Baker) DMF were transferred to a 25 mL three-necked flask which was flushed with a N_2 for 5 min. $Ru(DMSO)_4Cl_2$ and 4*p*-PTZ (2 equiv) were added to the flask. The reaction was heated to reflux for 90 min to yield a dark purple solution. This solution was cooled to room temperature, 50 mL of water was added, and the resulting emulsion was transferred to a separatory funnel. The aqueous layer was then repeatedly extracted with 50 mL portions of CH_2Cl_2 until little or no color remained. The purple CH_2Cl_2 fractions were combined and extracted with 4 × 50 mL of H_2O. The organic phase was dried with anhydrous Na_2CO_3, filtered, and reduced in volume by rotary evaporation to approximately 5 mL. 50 mL of ether was slowly added to this solution to precipitate the crude product as a fine gray-purple powder. The product was isolated by centrifugation, dissolved in CH_2Cl_2, and chromatographed on a short silica gel column (eluent CH_2Cl_2). Fractions containing the pure product were combined and concentrated by rotary evaporation to approximately 5 mL. 50 mL of ether was added slowly to precipitate the product as a fine purple powder. The product

was isolated by centrifuge and washed with 2 × 5 mL portions of ether. Typical yields after chromatography are 20−40%.

[Ru(44-PTZ)$_2$(DMB)](PF$_6$)$_2$. A red glass test tube containing a mixture of Ru(44-PTZ)$_2$Cl$_2$ (approximately 30 mg) in 15 mL of ethylene glycol under N_2 was placed in a paraffin bath at 120 °C for 30 min after which the solution was allowed to cool to room temperature. To the resulting red/orange solution, DMB (1 equiv) was added; and this solution was then placed in the 120 °C paraffin bath for 30 min. The solution was cooled to room temperature, diluted 1:1 with distilled water, and filtered. Aqueous NH_4PF_6 was added and the resulting orange solid collected by centrifugation. Column chromatography on silica gel (eluent 40% H_2O−10% KNO_3 (aq satd)−50% acetonitrile (4:1:5 (vol)) was used for purification. Acetonitrile was removed by evaporation from those fractions containing only the desired product (as determined by TLC) and aqueous NH_4PF_6 was added dropwise. Throughout the above procedure, light was rigorously excluded. The solid was filtered and washed with water (yields typically 20−40%).

[Ru(4*p*-PTZ)$_2$(423-DQ^{2+})](PF$_6$)$_4$ (XI). A red glass test tube containing a mixture of Ru(4*p*-PTZ)$_2$Cl$_2$ (approximately 30 mg) in 15 mL of ethylene glycol under N_2 was placed in a paraffin bath at 120 °C for 30 min after which the solution was allowed to cool to room temperature. To the resulting red/orange solution, (423-DQ^{2+})(PF$_6$-)$_2$ (1 equiv) was added and this solution was then placed in the 120 °C paraffin bath for 30 min. The solution was cooled to room temperature, diluted 1:1 with distilled water, and filtered. Aqueous NH_4PF_6 was added and the resulting orange solid collected by centrifugation. Column chromatography on silica gel (eluent 40% H_2O−10% KNO_3 (aq satd)−50% acetonitrile (4:1:5 (vol)) was used for purification. Acetonitrile was removed by evaporation from those fractions containing only the desired product (as determined by TLC) and aqueous NH_4PF_6 was added dropwise. Throughout the above procedure, light was rigorously excluded. The solid was filtered and washed with water (yields typically 20−40%). Electrospray mass spectroscopy provided parent molecular ion peaks for [Ru(4*p*-PTZ)$_2$(423-DQ^{2+})]$^+$(PF$_6$)$_3$ at 1791.1, 1846.5, 1874.5, 1902.6 for p = 4, 6−8 respectively.

[Ru(4*p*-PTZ)$_2$(424-DQ^{2+})](PF$_6$)$_4$ (XII) and [Ru(44-PTZ)$_2$-(4*m*4-DQ^{2+})](PF$_6$)$_4$ (XIII). These series of complexes were prepared in analogous fashion to the above series. Electrospray mass spectroscopy provided parent molecular ion peaks for [Ru(4*p*-PTZ)$_2$(424-DQ^{2+})]$^+$(PF$_6$)$_3$ at 1778.6, 1806.9, 1834.0, 1861.7, 1889.4, 1916.8 for p = 3−8 respectively.

Determination of Sample Integrity. Mass spectral analysis (*vida supra*) confirms that the structure of the D−C−A complexes are as reported. A combination of methods were employed to establish sample integrity (**XI**, **XII**, and **XIII**) for purposes of photophysical measurements. First, elemental analyses were previously obtained on these and related complexes. Unfortunately, elemental analysis has proven to be not especially useful in determining complex purity. For example, samples which have yielded entirely acceptable C, H, and N analysis values proved to be impure by electrochemical and spectral criteria and vice versa. The failure of classical elemental analysis in this context probably stems from a combination of the large molecular weight of the complexes (over 1700), the fact that they are noncrystalline salts, and the fact that they are unstable in the presence of both light and oxygen. In practice, a combination of chromatographic, electrochemical, and spectral analyses proved to be much more dependable in establishing sample integrity for time-resolved studies.

Samples were purified by repeated water-washed silica gel column chromatography [eluent 40% H_2O−10% KNO_3 (aq satd)−50% acetonitrile 4:1:5 (vol)] until they yielded constant UV−visible spectra which did not change with further chromatographic purification. Impure samples have broad adsorptions throughout the UV region and a shoulder at about 500 nm. Thus, the initial criterion of purity was the exact superposition of the spectrum throughout the UV and visible regions with scaled spectra of samples shown to be pure by electrochemistry, TLC, and static and time-resolved spectroscopy (*vide infra*).

After chromatographic purification, all samples were examined by cyclic voltammetry. Cyclic voltammograms of the complexes showed oxidation/reduction waves for various components of the system: two one-electron reductions of the diquat acceptor moiety, three one-electron reductions for the ruthenium chromophore moiety, and a two-electron oxidation for the (combined) two phenothiazine moieties. Each redox process had the correct potential and peak current ratios, and each was fully chemically reversible. Finally, in pure samples no other redox processes were observed within the potential range scanned.

In summary, a combination of thin layer chromatography, spectral analysis, and electrochemical analysis along with internal consistency of the kinetic data has proven to be a more consistent and dependable measure of sample integrity than more conventional analytical means.

Picosecond Kinetic Measurements. The amplified dye laser system employed in the 371 nm excite, 570 nm detect experiments is based on a dye laser synchronously pumped by an active/passive mode-locked Nd:YAG laser. The dye laser output is amplified in a three-stage amplifier which is pumped by an amplified, frequency-doubled, single-selected pulse from the YAG laser. The system has been described in detail previously.[11] Using the laser dye rhodamine 560, 570 nm light (5 ps, 200 μJ) pulses were generated and a small fraction used (<5 μJ) to probe the sample. Samples were excited with 371 nm light (5 ps, 60−70 μJ) pulses produced by mixing the 570 nm (5 ps, 200 μJ) pulse with a 1064 nm (30 ps, 150 μJ) pulse. The system used for 355 nm excite, 532 nm detect experiments is based on the same active/passive mode-locked Nd:YAG laser with a single-pulse selector and amplifier system. Samples were excited with the third harmonic 355 nm light (30 ps, 60−70 μJ) pulses. The samples were probed with second harmonic 532 nm light (30 ps, <5 μJ) pulses. The system has been described in detail previously.[6] Excitation beams were focused to a spot size of approximately 0.5 mm, and the probe beam employed was collinear with the excitation beam. A stepper motor driven variable delay controls the relative arrival time of the excitation and probe pulses. The arrival time of the probe pulses can be varied from −1 to 12 ns, relative to the arrival of the excitation pulse. The temporal instrument response function was determined by the convolution of the two 8 or 30 ps excitation and probe pulses and was ca. 10 or 45 ps fwhm. The excitation beam is separated from the probe beam through the use of Hoya Y48 and Y50 filters. Two beams, a probe and a reference, were collected on two EGG UV-100-BQ photovoltaics. The output of each photovoltaic was amplified, integrated, and digitized on each laser shot. Digital signals were stored in an IBM PC/AT computer, which also controls firing of the laser and movement of the delay stage.

The magnitude of the transient absorption signal depends on the sample concentration and on alignment of the excitation and probe beams at the sample as well as the extinction coefficients for the various transitions. Since the alignment of the two beams is impossible to reproduce day to day, it is not

TABLE 1: Reduction Potentials for PTZ-Linked Complexes (vs SCE)[a]

	Ru (3+/2+)	PTZ (+/0)	DQ (2+/+)	DQ (+/0)	Ru (2+/+)	Ru (+/0)
$Ru(DMB)_3^{2+}$	+1.13				−1.37	−1.54
Me-PTZ		+0.65				
422-DQ^{2+}			−0.43	−0.89		
432-DQ^{2+}			−0.64	−0.87		
424-DQ^{2+}			−0.77	−0.89		
$[Ru(44\text{-}PTZ)_2(422\text{-}DQ^{2+})]^{4+}$	+1.12	+0.70	−0.43	−0.88	−1.40	−1.59
$[Ru(43\text{-}PTZ)_2(423\text{-}DQ^{2+})]^{4+}$	+1.14	+0.74	−0.64	−0.87	−1.39	−1.59
$[Ru(44\text{-}PTZ)_2(423\text{-}DQ^{2+})]^{4+}$	+1.12	+0.70	−0.65	−0.88	−1.40	−1.58
$[Ru(45\text{-}PTZ)_2(423\text{-}DQ^{2+})]^{4+}$	+1.14	+0.69	−0.64	−0.89	−1.42	−1.59
$[Ru(46\text{-}PTZ)_2(423\text{-}DQ^{2+})]^{4+}$	+1.14	+0.70	−0.64	−0.87	−1.43	−1.58
$[Ru(47\text{-}PTZ)_2(423\text{-}DQ^{2+})]^{4+}$	+1.14	+0.70	−0.65	−0.86	−1.40	−1.59
$[Ru(48\text{-}PTZ)_2(423\text{-}DQ^{2+})]^{4+}$	+1.12	+0.69	−0.64	−0.88	−1.39	−1.60
$[Ru(43\text{-}PTZ)_2(424\text{-}DQ^{2+})]^{4+}$	+1.13	+0.75	−0.77	−0.87	−1.42	−1.58
$[Ru(44\text{-}PTZ)_2(424\text{-}DQ^{2+})]^{4+}$	+1.14	+0.69	−0.78	−0.89	−1.40	−1.58
$[Ru(45\text{-}PTZ)_2(424\text{-}DQ^{2+})]^{4+}$	+1.12	+0.70	−0.77	−0.88	−1.39	−1.59
$[Ru(46\text{-}PTZ)_2(424\text{-}DQ^{2+})]^{4+}$	+1.14	+0.70	−0.77	−0.87	−1.40	−1.57
$[Ru(47\text{-}PTZ)_2(424\text{-}DQ^{2+})]^{4+}$	+1.13	+0.69	−0.76	−0.90	−1.41	−1.59
$[Ru(48\text{-}PTZ)_2(424\text{-}DQ^{2+})]^{4+}$	+1.14	+0.70	−0.77	−0.87	−1.42	−1.60
$[Ru(44\text{-}PTZ)_2(424\text{-}DQ^{2+})]^{4+}$	+1.14	+0.70	−0.77	−0.88	−1.40	−1.58
$[Ru(44\text{-}PTZ)_2(434\text{-}DQ^{2+})]^{4+}$	+1.12	+0.69	−0.78	−0.88	−1.39	−1.58
$[Ru(44\text{-}PTZ)_2(444\text{-}DQ^{2+})]^{4+}$	+1.14	+0.70	−0.77	−0.89	−1.40	−1.59

[a] Acetonitrile solvent.

possible to compare the intensities of spectra. Absolute transient absorbances varied from 0.01 to 0.08 depending on the above variables.

Preparation of Samples for Kinetic Studies. Solid samples of all the complexes were either kept rigorously in the dark or stored in a dribox (Vacuum Atmospheres Corp.) under N_2 atmosphere to prevent decomposition in the presence of O_2. A small quantity (ca. 2 mg) was transferred to a sample tube, consisting of a 2 mm path length quartz cell attached to a Pyrex tube sealed with a Kontes Teflon-and-glass valve. Sample tubes were then evacuated on a vacuum line for about 5 min ($<5 \times 10^{-3}$ Torr). A portion of dichloroethane (Aldrich reagent grade) was then degassed by 4−5 cycles of freeze−pump−thaw and distilled over into a Pyrex side arm of the sample cell. Two more freeze−pump−thaw cycles were then performed, and the sample tubes sealed under vacuum. Sample absorbances generally ranged from 0.2 to 0.8 at 460 nm.

Results

Electrochemistry. The electrochemical waves of the D−C−A complexes, obtained by cyclic voltammetry, can be easily assigned by comparison with the waves that are observed for the separate, isolated components. Reduction potentials are presented in Table 1. Analysis of the voltammetric waves indicates the ratio of 2:1:1:1:1:1 for PTZ/PTZ^+, $diquat^{2+}diquat^+$, $diquat^+/diquat^0$, Ru^{2+}/Ru^+, Ru^+/Ru^0, and Ru^0/Ru^-, respectively, for the number of electrons in each process.

Ground-State Absorption Spectra. The static absorption spectra of $Ru(bpy)_3^{2+}$ complexes are characterized by intense bands in the UV and visible regions. The bands observed at about 300 nm correspond to bipyridine $\pi-\pi^*$ transitions. The band in the visible region corresponds to the Ru−bpy metal to ligand charge-transfer (MLCT) transition having a maximum absorption at about 460 nm. The donor (PTZ) and acceptor (DQ^{2+}) components do not absorb in the visible region; however, both the donor and the acceptor absorb in the UV. The DQ^{2+} moiety absorbs below 290 nm in both the coordinated and uncoordinated forms. The ligands containing a phenothiazine donor absorb below 330 nm when uncoordinated; and when coordinated in the D−C−A complexes a weak increased absorbance up to 390 nm is observed. This increased absorbance is independent of the chain length separating the donor and chromophore.

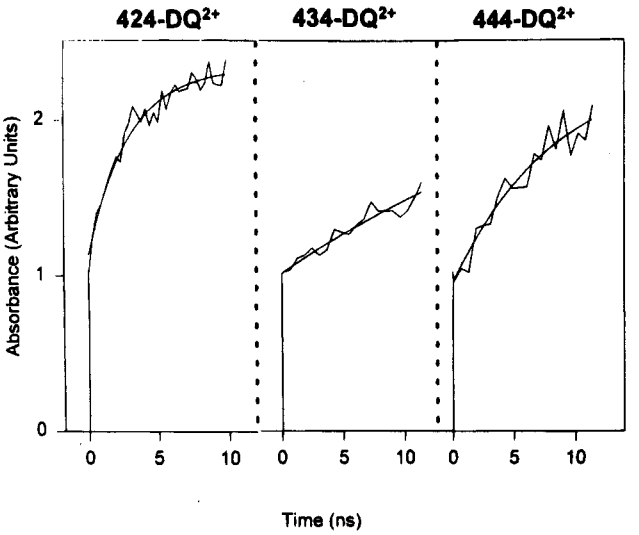

Figure 2. Transient absorption data and experimental fits for the series $Ru(44\text{-}PTZ)_2 4m4\text{-}DQ^{2+}$ in DCE; 355 nm pulse, 532 nm probe.

Transient Absorption Kinetics. Transient absorption kinetics were measured for the D−C−A complexes, $[Ru(4p\text{-}PTZ)_2(42n\text{-}DQ^{2+})]^{4+}$ ($p = 3-8$ and $n = 3, 4$) at different excitation and detection wavelengths. Absorbance kinetics of the donor−chromophore complex $[Ru(44\text{-}PTZ)_2(DMB)]^{2+}$ and *N*-methylphenothiazine were also obtained. The excitation wavelengths were 371 and 355 nm and the absorbance changes were detected at 570 and 532 nm, respectively. For the D−C−A complexes, both sets of wavelength conditions showed two components in the appearance kinetics, followed by a very slow (>20 ns) decay. The appearance kinetics obtained for the D−C−A complexes consist of a fast, pulse-width-limited components and a slower rise which can be fitted to a single exponential. Typical transients observed at 532 nm following 355 nm excitation for $[Ru(44\text{-}PTZ)_2(4m4\text{-}DQ^{2+})]^{4+}$ ($m = 2, 3, 4$) complexes in dichloroethane (DCE) are shown in Figure 2; rate constants and relative contributions of the fast and slow components are given in Table 2. Transient absorption results for $[Ru(4p\text{-}PTZ)_2(42n\text{-}DQ^{2+})]^{4+}$ ($p = 3-8$ and $n = 3, 4$) are listed in Table 3.

Transient absorption kinetics obtained for the D−C complex, $[Ru(44\text{-}PTZ)_2(DMB)]^{2+}$ and *N*-methylphenothiazine, are much simpler than in the D−C−A cases. The D−C complex, [Ru-

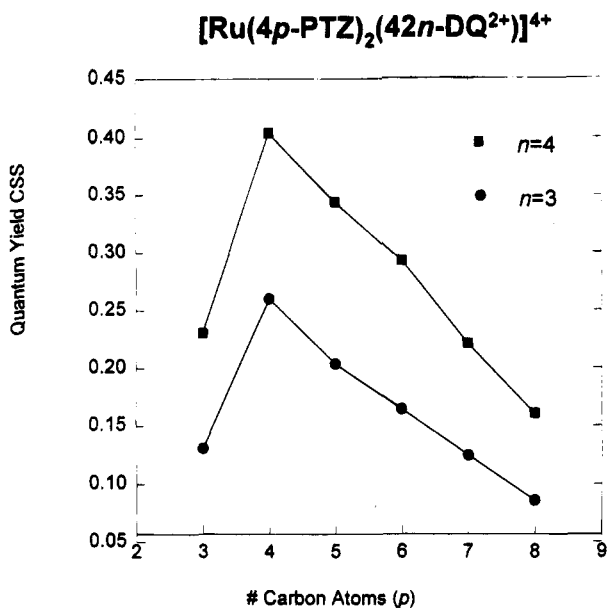

Figure 3. Quantum yield for charge separation vs the number of methylene units separating the donor and chromophore for the [Ru(4*p*-PTZ)$_2$(423-DQ^{2+})]$^{4+}$ and [Ru(4*p*-PTZ)$_2$(423-DQ^{2+})]$^{4+}$ series of complexes in DCE; 355 nm pulse, 532 nm probe.

(44-PTZ)$_2$(DMB)]$^{2+}$ and *N*-methylphenothiazine both exhibit a fast rise followed by a very slow decay in their transient absorption kinetics. The magnitude of this fast rise is roughly comparable to the magnitude of the fast rise observed in the D−C−A complex kinetics. We also note that the *N*-methylphenothiazine is totally nonluminescent in room temperature solution, presumably due to rapid intersystem crossing to the triplet manifold. The absorption observed in the *N*-methylphenothiazine 532 and 570 nm transient absorption kinetics is therefore assigned to a triplet-triplet absorption. On the basis of these observations, we assign the fast component observed for the D−C−A complexes to the direct n−π* excitation of the PTZ moiety resulting in PTZ* triplet−triplet absorption. At the 532 nm detection wavelength, in addition to the PTZ*, oxidized phenothiazine (PTZ$^+$) and reduced diquat (DQ$^+$) both have a significant absorbance (the ground state and the MLCT excited state do not). Thus, at the 532 nm probe wavelength the transient absorption results give the combined kinetics of PTZ* and the charge-separated state. At 570 nm, in addition to all of the same components which absorb at 532 nm, the MLCT excited state also has a significant absorbance.

In the case of the D−C−A complexes, the 532 nm absorbance shows little or no decay on the time scale of at least tens of nanoseconds. Preliminary transient absorption measurements in the nanosecond time regime indicate that each of the D−C−A complexes has a CS-state lifetime in the 100−200 ns range, which is consistent with previous published values for the [Ru(44-PTZ)$_2$(423-DQ^{2+})]$^{4+}$ complex.[5] Thus, the CS state decays completely by the next laser shot (300 ms).

Discussion

The synthetic scheme utilized results in the formation of a mixture of isomers of the D−C−A complexes. In principle, each of these could have different rate constants for certain transfer processes where electron-transfer distances vary from isomer to isomer. All of the electron-transfer processes discussed in this paper, however, involve the metal center and a single donor- or/acceptor-containing ligand. Thus the relevant electron-transfer distances are expected to be identical (or very nearly so) irrespective of the specific isomeric form of the complex. Consequently, the various isomers are not expected to have different rate constants for these processes. This argument is supported by the fact that the transient absorbance data fit well to single exponentials. In contrast, the various isomers would be expected to have different rate constants for electron transfers between oxidized donors and reduced acceptors (i.e., in recombination of the CS state) since the relevant electron-transfer distances for the various possible isomers are different. Not surprisingly, multiphasic kinetics are observed for the CS state recombination. These results will be discussed in a subsequent paper.

Assignment of the Fast Component. As mentioned above, the fast-rising portion of the transient absorption observed at 532 or 570 nm can best be rationalized in terms of direct photoexcitation triplet n−π* excited state. The phenothiazine moiety in the D−C−A complexes is attached via alkylation at the phenothiazine nitrogen; thus, its spectroscopy should be well approximated by the *N*-methylphenothiazine. Our results show that *N*-methylphenothiazine exhibits a triplet−triplet absorption at 532 and 570 nm. A similar, somewhat blue-shifted, triplet−triplet absorption has been reported previously for phenothiazine itself, i.e., no *N*-methyl group. In this case, the triplet state has been shown to have a lifetime of 1.5×10^{-4} s.[12]

We had speculated in an earlier publication on the origin, in the transient absorption kinetics, of the fast component at 532 and 570 nm.[6] At that time it was suggested that the fast component might be due to excitation of a charge-transfer complex formed between the chromophore and the phenothiazine donor which ultimately produced the same charge-separated state. More specifically, we speculated that excitation of this charge-transfer transition might initially produce RuL$_3^+$ and PTZ$^+$ and that these species would result in rapid (pulse width limited) formation of the charge-separated state. While such a process cannot be completely eliminated as a possible contributor to the fast component, a number of new observations suggest otherwise. The strongest evidence comes from transient absorption measurements on the series of chromophore−donor complex [Ru(44-PTZ)$_2$DMB]$^{2+}$. Here, again, a pulse width limited rise is observed, and the absorbance shows no detectable decay out to 10 ns (i.e., no evidence of forward or reverse of ET kinetics). Since this complex contains no electron acceptor it cannot form a long-lived charge-separated state. Furthermore, over a period of 10 ns an absorbance decay of Ru$^+$ and PTZ$^+$ would be expected since this back electron transfer is significantly exothermic. These D−C complexes do exhibit comparatively slow electron transfer following MLCT excitation, and their excited-state dynamics will be fully discussed in a later paper.[8]

While the assignment of the fast-rising component to direct PTZ n−π* excitation is not absolute, the absorbance is clearly PTZ based and is uniform for complexes containing a fixed number of PTZ moieties per molecule. Consistent with the above assignment, this fast component provides a convenient internal standard for relative quantitative analysis of transient absorbance data for the various complexes investigated here.

Mechanism of Charge Separation. As stated in the introduction above, emission lifetime studies of C−A complexes have previously been used to determine the oxidative quenching rates of the MLCT states in chromophore−acceptor analogs of the D−C−A systems.[4] In every case the emission decay kinetics of the C−A complexes and the appearance kinetics at 532 nm for the slow component in the D−C−A system are, within experimental error, identical. Furthermore, reductive quenching in C−D analogs recently has been shown to be much slower than emission quenching in the corresponding D−C−A

TABLE 2

complex[a]	magnitude[b] slow rise A_s	magnitude[b] fast rise A_f	slow rise time (ns)[d]	emission decay time (ns)	A_f/A_s	k_{rev}/k_2	quantum yield[c]
$[Ru(44\text{-}PTZ)_2(424\text{-}DQ^{2+})]^{4+}$	0.57	0.43	3.2	3.12	0.75	1.47	0.40
$[Ru(44\text{-}PTZ)_2(434\text{-}DQ^{2+})]^{4+}$	0.58	0.42	27.0		0.72	1.37	0.42
$[Ru(44\text{-}PTZ)_2(444\text{-}DQ^{2+})]^{4+}$	0.59	0.41	8.0		0.70	1.31	0.43

[a] 1,2-Dichloroethane solvent. [b] Magnitude of absorbance for the slow components were obtained from values extrapolated to 50 ns. [c] Quantum yields are calculated from relative values obtained from the A_f/A_s ratio assuming an absolute value for $[Ru(44\text{-}PTZ)_2(423\text{-}DQ^{2+})]^{4+}$ of 0.26 (ref 15). [d] The reported values are accurate within 15%.

TABLE 3

complex[a]	magnitude[b] slow rise A_s	magnitude[b] fast rise A_f	slow rise time (ns)[d]	emission decay time (ns)	A_f/A_s	k_{rev}/k_2	quantum yield[c]
$[Ru(43\text{-}PTZ)_2(423\text{-}DQ^{2+})]^{4+}$	0.30	0.70	0.90	0.96	2.33	6.94	0.13
$[Ru(44\text{-}PTZ)_2(423\text{-}DQ^{2+})]^{4+}$	0.47	0.53	0.90	0.96	1.23	2.85	0.26
$[Ru(45\text{-}PTZ)_2(423\text{-}DQ^{2+})]^{4+}$	0.40	0.60	0.90	0.96	1.50	4.10	0.20
$[Ru(46\text{-}PTZ)_2(423\text{-}DQ^{2+})]^{4+}$	0.35	0.65	0.90	0.96	1.86	5.32	0.16
$[Ru(47\text{-}PTZ)_2(423\text{-}DQ^{2+})]^{4+}$	0.29	0.71	0.90	0.96	2.45	7.35	0.12
$[Ru(48\text{-}PTZ)_2(423\text{-}DQ^{2+})]^{4+}$	0.22	0.78	0.90	0.96	3.55	11.05	0.08
$[Ru(43\text{-}PTZ)_2(424\text{-}DQ^{2+})]^{4+}$	0.43	0.57	3.00	3.20	1.33	3.34	0.23
$[Ru(44\text{-}PTZ)_2(424\text{-}DQ^{2+})]^{4+}$	0.57	0.43	3.00	3.20	0.75	1.46	0.40
$[Ru(45\text{-}PTZ)_2(424\text{-}DQ^{2+})]^{4+}$	0.53	0.47	3.00	3.20	0.89	1.91	0.34
$[Ru(46\text{-}PTZ)_2(424\text{-}DQ^{2+})]^{4+}$	0.49	0.51	3.00	3.20	1.04	2.41	0.29
$[Ru(47\text{-}PTZ)_2(424\text{-}DQ^{2+})]^{4+}$	0.42	0.58	3.00	3.20	1.38	3.52	0.22
$[Ru(48\text{-}PTZ)_2(424\text{-}DQ^{2+})]^{4+}$	0.35	0.65	3.00	3.20	1.90	5.22	0.16

[a] 1,2-Dichloroethane solvent. [b] Magnitude of absorbance for the slow components were obtained from values extrapolated to 50 ns. [c] Quantum yields are calculated from relative values obtained from the A_f/A_s ratio assuming an absolute value for $[Ru(44\text{-}PTZ)_2(423\text{-}DQ^{2+})]^{4+}$ of 0.26 (ref 15). [d] The reported values are accurate within 15%.

SCHEME 1

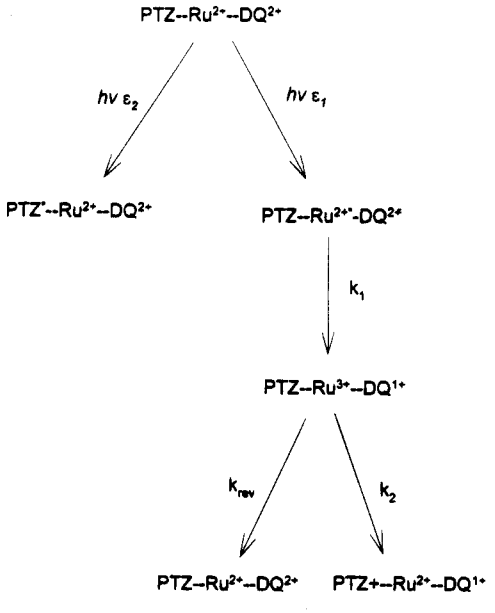

complexes.[8] Scheme 1 shows the proposed mechanism of charge-separated state formation, which is consistent with the above observations. Except for the formation of the PTZ* species under UV excitation, this scheme is the same as was demonstrated to be the case by multiwavelength transient absorption study reported previously.[6] Excitation results in population of both the MLCT state and PTZ (n, π^*) states. On the 10 ns time scale, PTZ excitation is a "dead end", and only the MLCT state participates in ET. The optical electron in the MLCT state resides in a π^* orbital localized on a single bipyridine ligand. Interligand electron transfer, however, in $Ru(bpy)_3^{2+*}$ complexes has been shown to be fast (<15 ps)[13] so that thermal equilibrium is established among the MLCT states on the three bipyridines prior to any chromophore-to-acceptor ET event. Thus, the MLCT quenching and the transient absorption kinetics at 532 nm can be described with a single rate constant, denoted k_1 in Scheme 1. Following this forward ET the Ru^{3+} either accepts an electron from the PTZ donor (k_2) or recombines with the reduced diquat acceptor to return to the ground state (k_{rev}). k_{rev} and k_2 are both at least an order of magnitude larger than k_1; and thus, the $PTZ^+-Ru^{2+}-DQ^+$ charge-separated state appears with the same kinetics as the MLCT state disappears.

Comparison of the amplitudes of the fast and slow components from the 355 nm excitation, 532 nm probe measurements for the D−C−A complexes allows the determination of the ratio of k_{rev} to k_2. Excitation at 355 nm produces several states: the MLCT state, the bipyridine $\pi-\pi^*$ state, the metal-based d−d* state, and the PTZ n−π^* state. In all but the last case the system quickly (<5 ps) relaxes to the MLCT state. Thus, the 355 nm extinction coefficient for MLCT state formation is the sum of the MLCT, d−d*, and $\pi-\pi^*$ spectroscopic extinction coefficients.

Both PTZ* and the CS state absorb at 532 nm. Since the MLCT state does not absorb at 532 nm, the fast component results entirely from PTZ* absorption. Thus, the relative magnitude of the fast component depends only in the extinction coefficient of the phenothiazine. The relative magnitude of the slow component depends on the extinction coefficient for MLCT state formation and also varies with the values of k_2 and k_{rev} in Scheme 1.

Quantitative estimates of how k_{rev} and k_2 change with various structure modifications can be made by comparing the amplitudes of the fast and slow components of the transient absorbance. An expression for the magnitude of the slow component is given by

$$A_s = \epsilon_1 \phi_{cs} = \epsilon_1 [k_2/(k_{rev} + k_2)$$

where ϵ_1 is the extinction coefficient for MLCT state formation and ϕ_{cs} is the quantum yield for formation of the charge-separated state. The amplitude of the fast component is given

as

$$A_f = \epsilon_2$$

The ratio of the two amplitudes is

$$A_s/A_f = (\epsilon_1/\epsilon_2)\phi_{cs} = \epsilon_1/\epsilon_2[k_2/(k_{rev} + k_2)]$$

or

$$A_f/A_s = \frac{\epsilon_2}{\epsilon_1}\left[1 + \frac{k_{rev}}{k_2}\right] \quad (1)$$

Thus, the relative values of k_{rev} and k_2 can be determined from the ratios of the slow to fast components. How the relative values of k_{rev} and k_2 vary with the length of the methylene linkage is discussed below.

Electron-Transfer Dependence on Acceptor Linkage. An important observation results from the comparison of the fast and slow components associated with [Ru(4,4-PTZ)$_2$(4*m*4-DQ^{2+})]$^{4+}$ (m = 2, 3, 4) D−C−A complexes. To obtain the fast to slow ratio, A_f/A_s, the magnitude of the fast absorbance component is compared with the extrapolated magnitude of the slow absorbance component (t > 3 lifetimes). The relative amount of the slow component (i.e., the amount of CS state ultimately formed) is *independent* of the value of m. Since for this series the pathway to the CS state involves the same donor (i.e., Ru(L)$_3^{3+}$ and 44-PTZ are the same in each case, thus, k_2 should not change), the back electron transfer rate, k_{rev}, must also be independent of the number of methylenes in the acceptor linkage, m. Again, this is in sharp contrast to the forward rate, k_1.

The absence of a C−A chain-length dependence for the back electron transfer has two important implications. *First, it is unlikely that the back electron transfer reaction is occurring through a superexchange mechanism involving the polymethylene σ framework.* If that were the case there should be a strong linkage dependence of k_{rev} over these three complexes, and there is not. Second, the lack of a linkage dependence in conjunction with the very rapid reverse ET rate suggests that the back electron transfer occurs on a time scale which is short relative to dynamics which control the chromophore−acceptor distances. Thus, reverse ET and, necessarily, the formation of the CS state; each occurs within the lifetime of an association complex formed during forward ET (k_1). In other words, it appears that the diquat and Ru(bpy)$_3^{2+*}$ achieve a conformation with appropriate orbital overlap and then forward electron transfer (MLCT quenching) takes place. Either back electron transfer or charge separation (phenothiazine to Ru^{3+} electron transfer) occurs immediately following MLCT quenching and before the reduced diquat can undergo cage escape.

The association complex mechanism proposed above has an additional implication. Since the back electron transfer appears to be independent of the acceptor linkage, the quantum yield for CS state formation is, as a result, also independent of chain length. Thus, there is no quantum yield advantage to increasing the chain length separating the ruthenium moiety and the diquat. While k_1 does depend on the acceptor linkage, the oxidative quenching rates for all D−C−A complexes having m < 7 are fast enough compared to nonradiative decay so that quantum yields for quenching of the MLCT state are greater than 90%. There may, therefore, be an advantage to increasing m in terms of the lifetime of the CS state without any penalty in terms of quantum yield to CS state formation. Nanosecond time scale experiments are planned in the near future to determine the dependence of CS state lifetime on acceptor and donor linkage.

Consideration of the data in Table 2 also reveals that the appearance rates of the CS state in the [Ru(44-PTZ)$_2$(4*m*4-DQ^{2+})]$^{4+}$ (m = 2, 3, 4) complexes, in DCE solvent do not decrease monotonically with increasing values of m, as might be expected. Rather, the fastest rate is seen in the 424-DQ^{2+} complex and the lowest in the 434-DQ^{2+} complex. Similar results have previously been observed by Schmehl et al.[10] in the MLCT quenching rates of a series of C−A complexes of the form Ru(L)$_2$(4*m*3-DQ^{2+})]$^{4+}$ (m = 2−7) in acetonitrile solvent. They observed that the trend in the rate of quenching with m for acceptors having even numbers of methylenes was different from those having odd numbers. In each series the rate decreased with increasing m; but, in general, the complexes with odd numbers of methylenes in the linkage quenched more slowly than those with even numbers. When both groups are considered together, the quenching rate actually oscillated for the shortest members of the series: namely, the quenching rates followed the order 423-DQ^{2+} > 443-DQ^{2+} < 433-DQ^{2+}.

Donor Linkage. In Scheme 1 the back electron transfer, k_{rev}, should be *independent* of the donor ligand (the PTZ) and *dependent* on the acceptor ligand (the diquat) since the reaction involves only Ru^{3+} and DQ$^+$. Likewise, k_2 should be *dependent* on the donor ligand and *independent* of the acceptor ligand since the reaction involves only Ru^{3+} and PTZ. Therefore, for a series of D−C−A complexes with a constant diquat acceptor and different donors, changes in the quantum yields for CS state formation should reflect only changes in k_2 (since k_{rev} should be constant). Table 3 includes CS state formation quantum yield data for the two series of D−C−A complexes, [Ru(4*p*-PTZ)$_2$-(423-DQ^{2+})]$^{4+}$ and [Ru(4*p*-PTZ)$_2$(424-DQ^{2+})]$^{4+}$, where p = 3−8. The two series differ in the identity of the diquat acceptor. As the chain length is increased from p = 4 to 8 the amount of CS state formed in each series decreases; consequently, the value of k_2 is decreasing with p. The p = 3 donor-containing complex in each series is slower than predicted by extrapolation of the p = 4−8 data. This result can be rationalized by differences in driving force and will be considered in more detail below.

As discussed in the previous section, the independence of k_{rev} on the acceptor linkage, m, implies that back electron transfer occurs on a time scale fast relative to DQ$^+$ motion. Since the quantum yield for CS state formation for these complexes is in the range of ca. 0.10−0.50 it must also follow that electron transfer between PTZ and Ru^{3+} must also be fast relative to conformational motions. Consequently, the spatial distribution of PTZ donors relative to the ruthenium moiety at the instant that MLCT quenching occurs must determine the amount of charge separation which occurs. The complexes in which the methylene chains separating the chromophore and the PTZ are shortest are expected to have the highest fraction of phenothiazines within the electron-transfer distance. As the chain length increases, the total spatial volume available to the PTZs increases, and thus there is a decrease in the probability that a given PTZ will be within electron-transfer distance with the correct orbital orientation when MLCT quenching takes place. As such, we suggest that PTZ to Ru^{3+} ET is not characterized by a single rate constant, k_2, but a distribution of rate constants associated with the distribution of PTZ/Ru^{3+} distances. Increasing the value of p results in decreasing the fraction of this distribution for which PTZ-to-Ru^{3+} ET can compete with reverse ET and that results in a lower effective value of k_2. The above discussion is quite reasonable, but at this point no direct evidence exists showing this distribution of rates.

As indicated above, complexes containing 43-PTZ do not follow the trend established by the 4*p*-PTZ, p > 3, compounds. The quantum yield for the 43-PTZ complexes are lower than

observed in analogous 44-PTZ-containing complexes. As shown in Table 1, the oxidation potentials of 43-PTZ ligand and coordinated 43-PTZ are 10 and 40 mV higher, respectively, than the $p = 4-8$ carbon chain length phenothiazine ligands. Thus, the driving force for the electron transfer from phenothiazine to $Ru(bpy)_3^{3+}$ is exothermic by 0.44 V for $p = 4-8$ but only by 0.40 V for $p = 3$. This reduced driving force is expected to lower the rate of k_2 and, correspondingly, offset the increase in k_2 expected from shortening the chain length for this ligand. (This assumes Marcus normal region, as opposed to inverted behavior, which is reasonable based on the observations that the driving force is comparable to the k_1 driving force, which exhibits Marcus normal region behavior.[4]) Likewise, the complex containing the 423-DQ^{2+} and a ligand with a single methylene unit separating the bipyridine and the phenothiazine (41-PTZ) shows a PTZ oxidation 100 mV higher than the $p = 4-8$ complexes. A driving force of 0.34 V is estimated; and the quantum yield observed is, within experimental error, the same as observed for the 44-PTZ-containing complex. The negative effect on the ET rate, k_2, as a result of decreased driving force, and the positive effect resulting from the shorter chain length both appear to affect the rate of charge separation, k_2, in a similar but opposite manner.

Driving Force Dependence of Electron Transfer. The two series of D−C−A complexes studied contain either a 423- or 424-DQ^{2+}. As can be seen in Table 1, the reduction potentials for these two diquats differ by 150 mV. This results in different driving forces for MLCT quenching (k_1) as well as back electron transfer (k_{rev}). As mentioned above, MLCT quenching has been shown to occur in the Marcus normal region.[4] We have previously reported that the rate of the back electron transfer decreases when the driving force increases, placing reverse electron transfer in the inverted region.[6] This phenomenon is observed again for complexes containing identical donor ligands (4*p*-PTZ) and different acceptor ligands (423-DQ^{2+} and 424-DQ^{2+}). For each value of p, k_2 is expected to be constant because only the chromophore and donor are involved; and these are identical for each pair. The rate of back ET (k_{rev}) is decreased in complexes containing the 424-DQ^{2+} acceptor compared to those containing the 423-DQ^{2+}. A comparison of $\ln(k_{rev}(423)/k_{rev}(424))$ for the five pairs of complexes ($p = 3-8$) gives values of 0.73, 0.67, 0.76, 0.74, 0.75, respectively, with an average of 0.74. From this average value the dependence of $\ln(k_{rev})$ on ΔG is determined to be about 4.0 eV^{-1}. This result can be compared to those of a number of researchers: Mallouk *et al.*[14] report a slope of approx. 5.0 eV^{-1} for the plot of $\ln(k_{rev})$ vs ΔG for a closely related C−A system. Meyer *et al.*[15] observed Marcus inverted region behavior for the series of compounds $[(4,4'\text{-}X_2\text{-bpy})Re(CO)_3(py\text{-}PTZ)]^+$ (X = OCH_3, CH_3, H, $CONEt_2$, CO_2Et) and report a $\ln(k_{rev})$ vs ΔG slope of 3.4 eV^{-1}. Schanze[16] et al. have studied reverse electron transfer in $[(4,4'\text{-}X_2\text{-bpy})Re(CO)_3((dimethylamino)benzoate)]^+$ with a similar dependence on ΔG to that which we observe.

We can attempt (unsuccessfully) to interpret these relative rates using classical Marcus theory. In general, the rates are given by

$$k_{rev} = A \exp(-\Delta G^{\ddagger}/RT) \qquad (2)$$

where A is a constant which can be taken to be the same for the 423-DQ^{2+} and 424-DQ^{2+} D−C−A series of complexes. The value of $\Delta G^{\ddagger}$ as given by Marcus theory

$$\Delta G^{\ddagger} = \frac{\lambda}{4}\left(1 + \frac{\Delta G}{\lambda}\right)^2 \qquad (3)$$

For each pair of complexes containing identical electron donor ligands the *difference* in driving force for back electron transfer between the 423-DQ^+ and 424-DQ^+ and $Ru(bpy)_3^{3+}$ is the same. Marcus theory (eqs 2 and 3) predicts a larger negative dependence on ΔG than observed in the above systems using any reasonable value for λ. We have recently explained these differences in terms of the role of high-frequency electron acceptor vibrations in highly energetic electron-transfer reactions.[6]

Solvent Dependence on Electron Transfer. Charge-separated states in these donor−chromophore−acceptor complexes are observed to form in the relatively nonpolar solvents (e.g., dichloromethane, DCE, and 1,2-difluorobenzene) but not in the more polar solvent, acetonitrile. This result can be qualitatively understood in terms of the Marcus inverted behavior observed for reverse ET, and eq 3, above. Solvent reorganization energies, λ, are expected to be larger in more polar acetonitrile than in DCE. For example, λ values of 1000 and 800 mV are obtained in acetonitrile and DCE, respectively, for the forward ($Ru(bpy)_3^{2+*}$-to-DQ^{2+}) ET.[4] Comparable values are expected for PTZ-to-$Ru(bpy)_3^{3+}$ and reverse ET reactions. In the inverted region an increase in λ results in a decrease in $\Delta G^{\ddagger}$ whereas in the normal region increasing λ increases $\Delta G^{\ddagger}$. (This is easily seen by differentiating $\Delta G^{\ddagger}$ (eq 3) with respect to λ). Thus, in DCE the smaller value of λ will decrease k_{rev} (inverted) and increase k_2 (normal) relative to their values in acetonitrile. As a result, donor-to-chromophore ET can effectively compete with reverse ET and thus form CS state only in the less polar (smaller λ value) solvents, DCE, dichloromethane, and 1,2-difluorobenzene.

We had previously hypothesized that this solvent dependence might be due to the difference in the work term associated with moving the charged acceptor (DQ^+) to the oxidized chromophore (Ru^{3+}) during back electron transfer. This term is not expected to be present in uncharged phenothiazine's electron transfer to the $Ru(bpy)_3^{3+}$. As a result, we suggested that the rate of back electron transfer in DCE might be less than that in acetonitrile as a result of this work term. The results obtained from the $[Ru(44\text{-}PTZ)_2(4m4\text{-}DQ^{2+})]^{4+}$, $m = 2, 3, 4$, complexes make this explanation seem unlikey if, as suggested above, the phenothiazine-to-$Ru(bpy)_3^{3+}$, k_2, and back electron transfer, k_{rev}, occur before the molecular components can move relative to each other. Since the change in distance separating the various redox components during CS/recombination is argued to be negligible, the work term is not expected to play a role. Thus, the primary solvent effect is the change in λ and, hence, $\Delta G^{\ddagger}$ in the reverse ET.

Conclusions

Several conclusion can be drawn from the above studies and may be summarized as follows: The primary quenching mechanism of the MLCT state is chromophore to acceptor (diquat) electron transfer. Following MLCT quenching the D−C−A complexes may undergo either acceptor-to-chromophore or donor-to-chromophore electron transfer. It is the competition of these two process which determines the quantum yield for charge-separated state formation. We find that the rate of reverse electron transfer is independent of the length of methylene chain separating the chromophore and acceptor moieties. This argues against a superexchange electron-transfer mechanism involving the σ-bond linkages and suggests that reverse electron transfer occurs immediately following chromophore-to-acceptor electron transfer prior to large-amplitude motions. Since donor-to-oxidized-chromophore electron transfer competes with reverse electron transfer, we conclude that this process is also very fast.

The quantum yield for charge-separated state formation depends upon the length of the methylene chain separating the donor and chromophore moieties. This result is interpreted in terms of the fraction of donor moieties which are, at the instant of excited chromophore-to-acceptor electron transfer, sufficiently close to the chromophore for donor-to-chromophore electron transfer to occur.

The rate of reverse electron transfer is observed to decrease with increasing energetic driving force. This is interpreted in terms of Marcus inverted behavior and may be semiquantitively understood in terms of high-frequency quantized accepting vibrational modes.

Acknowledgment. This work was supported by (C.M.E.) U.S. Department of Energy, Office of Basic Energy Sciences (DE-FG02-92ER14301), and (D.F.K.) National Science Foundation.

References and Notes

(1) *Photoinduced Electron Transfer*; Fox, M. A., Chanon, M., Eds.; Elsevier: Amsterdam, 1088, and text references therein.

(2) Gust, D.; Moore, T. A. *Science* **1989**, *244*, 35.

(3) Gust, D.; Moore, T. A.; Moore, A. L.; Leggett, L.; Lin, S.; DeGraziano, J. M.; Hermant, R. M.; Nicodem, D.; Craig, P.; et al. *J. Phys. Chem.* **1993**, *97*, 7926−31 and text references therein.

(4) Cooley, L. F.; Larson, S. L.; Elliott, C. M.; Kelley, D. F. *J. Phys. Chem.* **1991**, *95*, 10694.

(5) Danielson, E.; Elliott, C. M.; Merkert, J. W.; Meyer, T. J. *J. Am. Chem. Soc.* **1987**, *109*, 2519.

(6) Larson, S. L.; Cooley, L. F.; Elliott, C. M.; Kelley, D. F. *J. Am. Chem. Soc.* **1992**, *114*, 9504.

(7) Johnson, D. G.; Niemczyk, M. P.; Minsek, D. W.; Wiederrecht, G. P.; Svec, W. A.; Gaines, G. L., III; Wasielewski, M. R., *J. Am. Chem. Soc.* **1993**, *115*, 5692−701 and text references therein.

(8) Larson, S. L.; Elliott, C. M.; Kelley, D. F., manuscript in preparation.

(9) Sawer, D. T.; Roberts, J. L. *Experimental Electrochemistry for Chemists*; Wiley: New York, 1974.

(10) Schmehl, R. H.; Ryu, C. K.; Elliott, C. M.; Headford, C. E. L.; Ferrere S. *Adv. Chem. Ser.* **1989**, *228*, 211.

(11) Swinney, T. C.; Kelley, D. F. *J. Chem. Phys.* **1993**, *99*, 211.

(12) Iwaoka, T.; Kokubun, H.; Koizumi, M. *Bull. Chem. Soc. Jpn.* **1971**, *44*, 341.

(13) Malone, R. A.; Kelley, D. F. *J. Chem. Phys.* **1991**, *95*, 8970.

(14) Yonemoto, E. H.; Riley, R. L.; Kim, Y. I.; Atherton, S. J.; Schmehl, R. H.; Mallouk, T. E. *J. Am. Chem. Soc.* **1993**, *115*, 5384.

(15) Chen, P.; Duesing, R.; Graff, D. K.; Meyer, T. J. *J. Phys. Chem.* 1991, *95*, 5850 and references therein.

(16) MacQueen, D. B.; Schanze, K. S. J. *Am. Chem. Soc.* **1991**, *113*, 7470.

JP942243H